Enhancement of Mass Transfer Using Piezoelectric Material in Fluid Flow System

Gi-Beum Kim*, Woo-Suk Chong**, Tae-Kyu Kwon*, Chul-Un Hong*, Nam-Gyun Kim*, Gyeong-Rak Jheong***

*Division of Bionics and Bioinformatics, College of Engineering, Chonbuk National University, Chonju, Korea
(Tel : +82-63-270-2246, E-mail : kgb70@mail.chonbuk.ac.kr)
**Department of Medical Engineering, Chonbuk National University, Chonju, Korea
(Tel : +82-63-270-4063, E-mail: biosuk@korea.com)
*Division of Bionics and Bioinformatics, College of Engineering, Chonbuk National University, Chonju, Korea
(Tel : +82-63-270-4066, E-mail : kwon10@chonbuk.ac.kr)
*Division of Bionics and Bioinformatics, College of Engineering, Chonbuk National University, Chonju, Korea
(Tel : +82-63-270-4065, E-mail : cuhong@chonbuk.ac.kr)
*Division of Bionics and Bioinformatics, College of Engineering, Chonbuk National University, Chonju, Korea
(Tel : +82-63-270-4061, E-mail : ngkim@chonbuk.ac.kr)
*** School of Chemical Eng., College of Engineering·The Research Center of Industrial Technology, Engineering Research Institute, College of Engineering, Chonbuk National University, Chonju, Korea
(Tel : +82-63-270-2436, E-mail : jheonggr@chonbuk.ac.kr,)

Abstract: The purpose of this work was to assess and quantify the beneficial effects of long-term gas exchange, at varying frequencies, for the development of a vibrating intravascular lung assistance device (VIVLAD), for patients suffering from acute respiratory distress syndrome (ARDS). The experimental design and procedure have been applied to the construction of a new device for assessing the effectiveness of membrane vibrations. An analytical solution has been developed for the hydrodynamics of flow through a bundle of sinusoidally vibrated hollow fibers, with the intention of gaining insight into how wall vibrations might enhance the performance of the VIVLAD. As a result, the maximum oxygen transfer rate was reached at the maximum amplitude and through the transfer of vibrations to the hollow fiber membranes. The device was excited by a frequency band of 7Hz at various water flow rates, as this frequency was the 2nd mode resonance frequency of the flexible beam. 675 hollow fiber membranes were also bundled, within the blood flow, into the device.

Keywords: Artificial lung, Gas transfer, PZT actuator, Acute Respiratory Distress Syndrome (ARDS)

1. INTRODUCTION

Acute respiratory distress syndrome (ARDS) is a form of acute respiratory failure caused by extensive lung injury following a variety of catastrophic events such as shock, severe infection, or burns. ARDS can occur in individuals with or without previous lung disease. People whose normal lungs have been injured, such as from exposure to noxious gases, steam, or heat during a fire, can subsequently go into respiratory failure.

Especially, respiratory failure usually occurs following a catastrophic event in individuals with no previous lung disease, not responding to ordinary methods of respiratory support. Regardless of the event causing the lung injury, the patients exhibit common signs and symptoms, x-ray findings, and tissue changes. Because many of its features resembled those of respiratory distress syndrome(RDS) in newborns, the adult disease is referred to as ARDS.

The disease affects approximately 150,000 people per year in the United States [1]. Its treatment requires respiratory support using the conventional therapies of mechanical ventilation, or extracorporeal membrane oxygenation (ECMO) in patients with severe ARDS. The positive airway pressures and volume excursions associated with mechanical ventilation can result in further damage to lung tissue, including barotrauma, volutrauma and parenchyma damage due to the toxic levels of oxygen required for effective mechanical ventilation [2]. The alternative use of ECMO is complicated and expensive, requiring extensive blood/biomaterial contact in extracorporeal circuits, systemic anticoagulation, and labor-intensive patient monitoring. Due to these complications, the mortality rate of ARDS patients remains high, exceeding 50% [3-9].

Intravascular oxygenation represents an attractive, alternative support modality for patients with ARDS. The concept of intravascular oxygenation as an alternative ARDS therapy originated with Mortensen [10], who developed an intravenous oxygenator (IVOX) consisting of a bundle of crimped hollow fiber positioned in the vena cava. In clinical trials, the IVOX provided an average of 28% of the basal gas exchange requirements for patients with severe ARDS [11]. The clinical study, however, concluded that more gas exchange was needed for intravascular oxygenation to be clinically effective in ARDS treatment. Herein, an intravenous membrane oxygenator was developed, with a design goal of 50% of the base oxygen and carbon dioxide exchange requirements for end-stage ARDS patients. Similarly to IVOX, the intravenous membrane oxygenator consists of a bundle of manifold hollow fiber, and is intended for intravenous placement within the superior and inferior vena cava. Due to the target level of gas exchange required in the intravenous membrane oxygenator, the intravenous membrane oxygenator consequently incorporates a vibrating actuator concentric with the fiber bundle, thus enhancing the gas exchange. Our current efforts focused on device improvements intended to provide the target levels of gas exchange, taking into account the constraints imposed by intravenous placement on the fiber bundle size, and hence the fiber area, for gas exchange. Although critical care techniques have been improved, the high mortality of severe acute respiratory failure (ARDS) has not significantly changed [12, 13].

In an intravenous membrane oxygenator, the greater part of the oxygen transfer resistance is located in the blood-side laminar film [14], and various methods have been tried to make the laminar film thinner and improve the oxygen transfer rate [15,16]. In the present study, the water flow

characteristics in the implantable artificial lung were evaluated by in vitro experiments methods [17].

The purpose of this study was to investigate the effect of vibration device in gas transfer rate for usage as intravacular lung assist device. Specific attention was focused on the effect of membrane vibration. Quantitative experimental measurements were performed to evaluate the performance of the device, and to identify membrane vibration dependence on hemolysis. Scaling analysis was then used to infer the dimensionless groups that correlate the performance of a vibrated hollow tube membrane oxygenator. The experimental design and procedure are then given for a device for assessing the effectiveness of membrane vibrations.

In this paper, an analytical solution were developed for the hydrodynamics of the flow through a bundle of sinusoidally vibrated hollow fibers to provide some insight into how wall vibrations might enhance the performance of an intravascular lung assist device. Scaling analysis was then used to infer the dimensionless groups that correlate the performance of a vibrated hollow tube membrane oxygenator. The experimental design and procedure are then given for a device for assessing the effectiveness of membrane vibrations.

2. THEORY

For the Reynolds numbers, the dimensionless rate of mass transfer, *K*, is given by

$$K = N_{\mathrm{Sh}} N_{\mathrm{Sc}}^{-1/3} = \alpha N_{\mathrm{Re}}^{\beta} \tag{1}$$

The Reynolds number, N_{Re} (=dv/υ), characterizes the flow regime and is the ratio of the inertial to viscous forces. The Schmidt number, N_{Sc} (=υ /*D*), analogous to the Prandtl number in heat transfer, characterizes the fluid properties and is to ratio of momentum to diffusive transports. The Sherwood number, N_{Sh} (=*Kd/D*), also known as the mass transfer Nusselt number, likewise characterizes the relative importance of the convective and diffusive transports; it is the ratio of the total to diffusive transports. In the above definitions, *d* is the characteristic length, *v* the velocity, *D* the diffusivity, υ the kinematic viscosity and *K* the mass transfer rate [18-21].

Characteristic length is given by

$$d = \frac{\varepsilon}{1-\varepsilon} d_o \tag{2}$$

in which ε is the device porosity and d_o the outside diameter of hollow fiber membrane.

The O_2 content and O_2 transfer rate were calculated by the following standard formulas:

$$\mathrm{O_2\ content(vol\%)} = \frac{\mathrm{Hb} \times 1.34 \times \%\mathrm{O_2\ saturation}}{100} \times P_{\mathrm{O_2}} \times 0.003 \tag{3}$$

$$\mathrm{O_2\ transfer\ rate(ml/min)} = (\mathrm{C_{aO_2}} - \mathrm{C_{vO_2}}) \times \text{liquid flow rate} \tag{4}$$

in which Hb is the hemoglobin and $P_{\mathrm{O_2}}$ the partial pressure of oxygen, with 1.34 and 0.003 the ml of oxygen that could be carried by 1mg of hemoglobin, and that dissolved for each 1mmHg, respectively, and $\mathrm{C_{aO_2}}$ and $\mathrm{C_{vO_2}}$ the arterial and venous oxygen contents, respectively; the blood flow rate represents the pump flow rate (L/min).

Blood hemolysis was expressed as Normalized Index of Hemolysis (NIH) according to the equation [22-24]:

$$\mathrm{NIH(g/100L)} = \frac{\Delta \mathrm{fHb} \times \mathrm{V} \times (1 - \frac{\mathrm{Ht}}{100}) \times 100}{\Delta \mathrm{t} \times \mathrm{Q}} \tag{5}$$

where, ΔfHb is the increase in free plasma hemoglobin concentration during the testing time, Ht is the hematocrit, V the blood volume of each circuit and Q the flow rate expressed in L/min.

3. Materials and Methods

3.1 Blood Condition

The blood was obtained from cattle having normal body temperature, no physical signs of disease, including diarrhea or rhinorrhea, and an acceptable range of hematological profiles. The blood is collected by vascular puncture using a 14G needle, and put into 500mL blood bags containing a citrate phosphate dextrose adenine (CPDA-1) anticoagulant solution.

Table1 Inlet parameters recommended by AAMI/ASTM Standard: Admitted range, minimum and maximum values measured during the test.

	AAMI recommended range	Measured		
		Average	Min.	Max.
T (℃)	37±1	37.0	36.8	37.2
B.E. (mmol/L)	0±5	1.1	-1.8	2.7
SvO2 (%)	65±5	65.5	64.0	68.0
Hb (g/dL)	12±1	12.0	11.6	12.5

Before testing, the blood was examined to check for damaged samples. As shown in Table 1 the initial mean free hemoglobin concentration was 5.33±2.75㎎/dL, and the mean hematocrit 28.1±3.0%. The blood was stored in a refrigerator during transportation and kept refrigerated upon arrival at our laboratory. All of the units of blood were used within 6 hours of acquisition.

3.2 Membrane Oxygenator

In this study, the experimental data were measured to evaluate the performance of the Vibrating Intravacular Lung Assist Device (VIVLAD). The test section was a cylinder duct with an axial length and inner diameter of 60 and 30 mm, respectively.

Figure 1 shows a photograph of the VIVLAD. The VIVLAD used for this experiment was prepared with the number of hollow fiber in the acryl cylinder as shown in Fig. 2. The VIVLAD was made of microporous polypropylene with an inner diameter and membrane thickness of 380 μm and 50 μm (Oxyphane, Enka, Germany), respectively. The experimental set-up of the flexible beam used in the artificial lung device is shown in Figure 2. The PVDF sensor was a 28 μm thickness LDT1-028K (AMP Co.). The piezoceramic sensor used for the test module was a multi-layer bender PZT actuator which was a PL-128.255 Lead Zirconate Titanate (PZT) from Digtal ECHO company.

The dimension was 40×10×0.45 mm. The PZT actuator and PVDF sensor were bonded to the flexible beam with araldite adhesive, with the electrical leads soldered to the electrode of piezo-elements, and then covered with elastic rubber for waterproofing. The description of the VIVLAD is shown in Table 2.

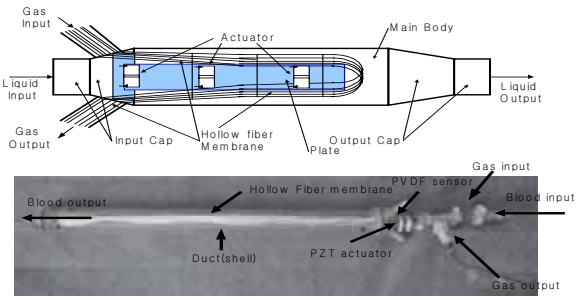

Fig.1 Vibrating intravenous lung assist device (VIVLAD).

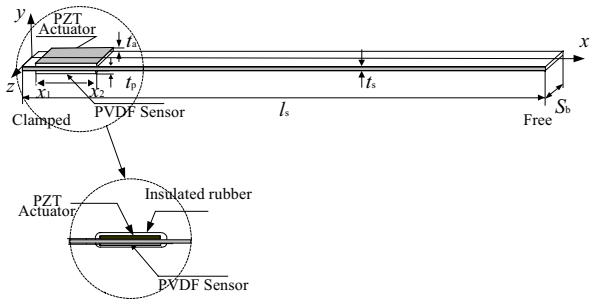

Fig.2 Configuration of a cantilevered composite beam with piezo-film sensor and piezo-ceramic actuator.

Table2 Dimensions of hollow fiber modules.

Parameter	Type 1	Type 2	Type 3	Type 4	Type 5
Membrane	Hollow fiber	Hollow fiber	Hollow fiber	Hollow fiber	Hollow fiber
Material	PP	PP	PP	PP	PP
Cylinder Duct Inner Diameter (mm)	30	30	30	30	30
Number of Hollow fiber	100	200	300	450	675

3.3 Measurements

The measurements were performed by the AAMI/ISO international standard recommendations [25]. The experimental closed loop was primed with less than 6 liters of fresh filtered cattle blood after addition of 75 ml ADC and 1 ml heparin as anticoagulants. The hemoglobin content was calibrated to the required value (12.0±1.0 g/dl) by dilution of the blood with normal saline. Adequate recirculation was performed before the test, to adjust the blood's inlet conditions to those of the AAMI/ISO standards (Table. 1). The test lasted six hours. Gas flow rates of up to 6 L/min through the 120-cm-long hollow fibers have been achieved by exciting a piezo-vibrator with a sinusoidal wave magnitude of DC 50 V. Figure 3 shows the experimental setup of the testing equipment for measurement of the blood oxygen transfer.

The experimental closed loop blood circuit consisted of 3/8 inch inner diameter biocompatibility tubing, a deoxygenator (Baxter Healthcare Corporation, Irvine, CA, USA), an electromagnetic blood flow meter and a roller pump (Cobe Cardiovascular, Inc., Arvada, Co. USA), which were used as the membrane oxygenator for this work. A gas blender (Sechrist Industries, Inc., Anaheim, CA) was connected to the deoxygenator with tube. The blood temperature was maintained at 37℃ with a heat exchanger.

Fig. 3 Experimental circuit for the evaluation of oxygen transfers with bovine blood.

The signal processing of the data was carried out using a DSP 1104 board (TMS320C40, dSPACE GmbH, Germany) and an amplifier (SQV 3/150, Pizomechanik Dr. L. Piekehman GmbH, Germany). The signal from an A/D converter, with a sampling ratio of 1ms, was sent to the DSP system and the calculated input voltage to a PZT actuator, for exciting the test module through the D/A converter and amplifier. The signals from the sensor, according to the applied input voltage, were digitalized and filtered in order to obtain the dynamic characteristics of the composite beam in the artificial lung device. In the filtering operation, the DC offset was rejected and the noise eliminated by band-pass filters (BPF) with the cutoff frequencies of 0.5 and 50Hz, respectively. Finally, the signals are integrated to take into account the applied input voltage. The processed signals of the sensor output were obtained in real time on a personal computer.

Experiments were performed with various frequencies applied to the PZT actuator of the test module, which was bonded to the flexible beam in the artificial lung device. The dynamic response of the sensor system was obtained by applying the dynamic input voltage with varying frequencies of sinusoidal wave, from 0 to 50 Hz, and magnitudes of the excited input from 0 to 100V. The measuring system was discredited at sampling intervals of 0.001s. Every hour, excitation of the test module frequency, f was varied, spanning 0 to 10Hz (step 1Hz), in four runs of 60 minutes each. In each tests, three veno-arterial blood samples were experimented and immediately analyzed.

The test VIVLAD was ventilated with 100% O_2, at a flow rate one time that of the blood flow. Samples were taken from the inlet and outlet sampling ports, and the blood gases analyzed with an i-Stat Portable Blood Gas/Electrolyte Analyzer (i-Stat Co., East Windser, NJ, USA). The O_2 and CO_2 transfer rates were calculated from the gas analysis data and blood flow rates. The data collection consisted of

recordings of the venous and arterial oxygen saturation values (SvO_2, SaO_2), oxygen partial pressure (pvO_2, paO_2), venous and arterial pH, and total hemoglobin (Hb) in the exhausted gas.

4. RESULTS AND DISCUSSION

Figure 4 shows the relationships between the oxygen transfer and various blood flow rates without an excited vibration. When the blood flow rate increases, the oxygen transfers rate increases, and the module type 5 showed a higher oxygen transfer rate than any other modules. In addition, the pressure drop in the intravenous artificial lungs assist must keep lower than 15 ㎜Hg. Therefore, when the blood flow rate was 6 L/min, there were 675 hollow fibers in the cylinders available for insertion, with an inner diameter of 3 ㎝.

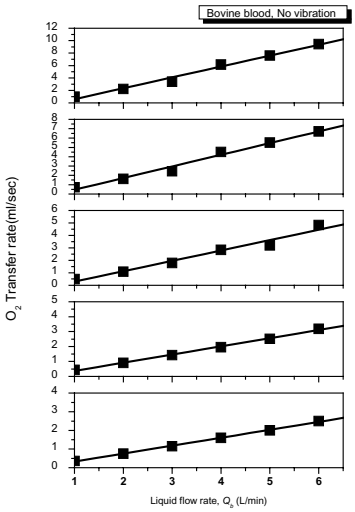

Fig.4 Oxygen transfer rate for the VIVLAD, with various module types and liquid flow rates, using bovine blood, with no vibration.

Figure 5 shows the relationships between the excited frequency and oxygen transfer rate on the blood flow rate with the various module types. When the excited frequency increases, the oxygen transfer rate increases. However, although the oxygen transfer rate of propagation expressed a maximum when frequency was 7Hz, with frequencies greater than 7Hz the oxygen transfer rate of propagation again show decreasing tendencies. The reason for this could be judged and confirm from Figure 5, where the frequency of 7Hz expressed a maximum oxygen velocity of propagation as the maximum flicker occurred in the blood of the fluid system. The maximum oxygen transfer rate seemed to be caused by the occurrence of the maximum amplitude and transfer of vibration to the hollow fiber when excited by a frequency of 7Hz for each blood flow rate, because this frequency became the 2nd mode resonance frequency of the flexible beam in blood flow.

Figure 6 shows the output voltage of the PVDF sensor at the maximum oxygen transfer rate in module type 4. As shown in this figure, the maximum amplitude of the PVDF sensor output was at a frequency band of 7Hz for various blood flow rates. The maximum oxygen transfer effect occurred at the frequency band of 7Hz. This resonance effect represented the maximum oxygen transfer rate by reducing the boundary layer, occurring on the surface of the hollow fiber membrane.

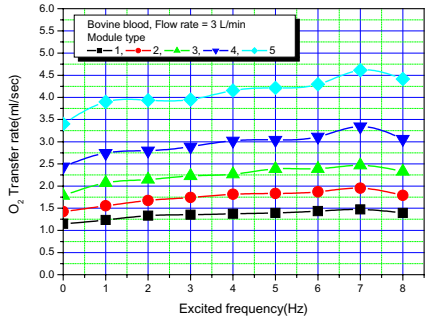

(a)

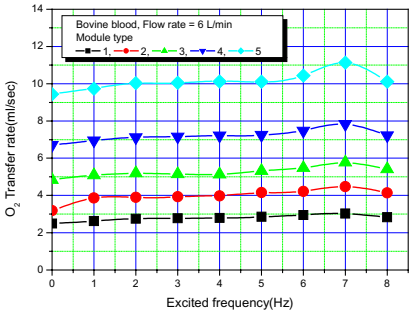

(b)

Fig. 5 Experimental circuit for the evaluation of the oxygen transfer in bovine blood. Oxygen transfer rate for the various VIVLAD module types, with the liquid flow rate varied, using bovine blood at various excited frequencies. (Blood flow rate (a) 3l/min, (b) 6l/min).

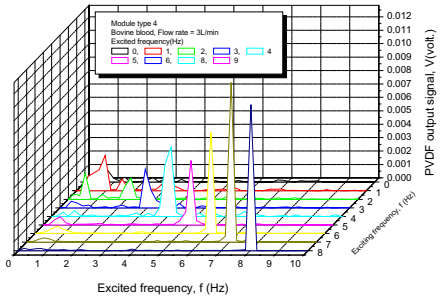

(a)

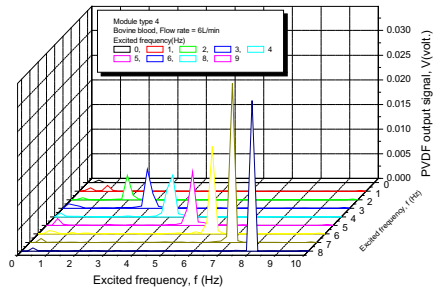

(b)

Fig.6 Amplitude of PVDF sensor output for the system with various excited frequencies using bovine blood

Figure 7 shows the dependence of the mass transfer rate K of the blood flow in the VIVLAD at various excited vibrations. The mass transfer rate increased with the linear velocity of the blood flow. A lower number of tired hollow fibers produce a higher mass transfer rate at a constant blood-side flow velocity. These results indicate that the packing of hollow fiber strongly affects the mass transfer rate. This figure is a log-log plot of K vs. N_{Re} for the experiment using the VIVLAD by varying the numbers of tied hollow fibers.

Least-squares fits yield the following equations:

$$K = \alpha N_{\mathrm{Re}}^{\beta}$$

$$\alpha = y_0 + Ae^{-f/t} \qquad (5)$$

$$y_0 = 0.52 + 58.47e^{-P^*/0.03}$$

$$A = -0.07 - 5.47e^{-P^*/0.04}$$

$$t = 2.48 + 0.0001e^{-P^*/0.22}$$

$$\beta = A' + B'x \qquad (6)$$

$$A' = 0.98 - 0.31e^{-p^*/0.02}$$

$$B' = 0.004 - 0.012p^*$$

These values for the slope and vertical position are used in the equation $K = \alpha N_{\mathrm{Re}}^{\beta}$ to predict the O_2 transfer rates in water for the VIVLAD with various numbers of tied hollow fibers.

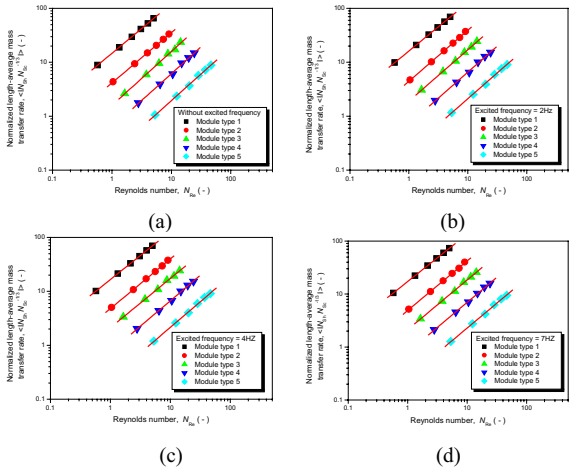

Fig.7 Oxygenation performance of the various VIVLAD module types, using bovine blood, at various excited frequencies. ((a) without exciting, (b) 2Hz, (c) 4Hz and (d) 7Hz)

Figure 8 shows the relationship between the changes in the plasma free hemoglobin and time at different flow rates in module type 5, indicating the maximum oxygen transfer rate. Figure 8 shows the changes in the plasma free hemoglobin with each PZT actuator activated with a sinusoidal wave amplitude of DC10V. The change in the plasma free hemoglobin was 0.112g/dL after 6 hours with a sinusoidal wave amplitude of DC10V and an excited frequency band of 7Hz at the blood flow rate of 5L/min in module type 5. From the results of hemolysis, it was determined that damage to blood does not occur because the hemolysis is low, which was measured during the 6 hours of excitation in frequency region of 7Hz in the experiment. Enhancing the performance of the contactors using the membrane vibrations also offers an additional advantage of minimizing fouling. Employing membrane vibrations may be more amenable to enhancing the performance of an implantable blood oxygenator because it is easier to implement and is less traumatic than when employing direct pulsations of the fluid flow.

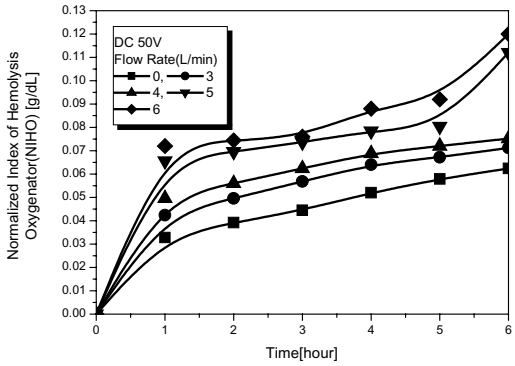

Fig.8 Graph reveals variation in the plasma free hemoglobin with various blood flow rates over the passage of time at an excited frequency of 7Hz

5. Conclusions

This study represents the limit of hemolysis, which is produced by the vibration techniques used to improve the oxygen transfer efficiency in the new type artificial lung assist device.

When the inner diameter of the module was 3cm, the hollow fiber membrane length was 120cm, and the maximum number inserted in the hollow fiber membranes was 675. The blood hemolysis was low in the frequency band of 7Hz, which had a maximum value for the oxygen transfer rate. The results reported above strongly indicate that mass transfer almost always controls the performance of microporous hollow-fibers in the blood phase. The oxygen transfer rate of the VIVLAD increased with increases in the number of tied hollow fibers, due to the more effective blood contact with the membrane.

The water flow in the VIVLAD was not uniform and depended on the hollow fiber packing density. The stagnation of the water flow also occurred in the bundle of hollow fibers at the water inlet.

ACKNOWLEDGMENTS

This study was supported by a grant of the Korea Health 21 R & D Project; Ministry of Health & Welfare, Republic of Korea (02-PJ3-PG6-EV05-0001).

REFERENCES

[1] F. L. Fazzalari, R. H. Bartlett, M. R. Bonnel and J. P. Montoya, "An Intrapleural Lung Prosthesis: Rationale, Design and Testing," *Artif. Organs*, vol. 18, no. 11, pp. 801, 1994.

[2] S. E. Weinberger, *Principles of Pulmonary Medicine*. Philadelphia, Saunders, 1992.

[3] L. Gattinoni, A. Pesenti and G. P. Rossi, "Treatment of acute respiratory failure with low-frequency positive-pressure ventilation and extracorporeal removal of CO2," *Lancet* , vol. 2, pp. 292-294, 1980.

[4] S. Ichiba, R. H. Bartlett, "Current status of extracorporeal membrane oxygenation for severe respiratory failure," *Artif. Organs*, vol. 20, pp. 120-123, 1996.

[5] A. Pesenti, L. Gattinoni, T. Kobolow and G. Damia, "Extracorporeal circulation in adult respiratory failure," *ASAIO Trans*., vol. 34, pp. 43-47, 1988.
[6] M. T, Snider, D. B. Campbell, W. A. Kofke, K. M. High, G. B. Russell, M. F. Keamy and D. R. Williams, "Venovenous perfusion of adult and children with severe acute respiratory distress syndrome," *ASAIO Trans*., vol. 34, 1014-1020, 1988.
[7] T. G. Campell, "Changing criteria for the artificial lung: Historic controls on the technology of ECMO," *ASAIO J*., vol. 40, pp. 109-120, 1994.
[8] W. J. Fedespiel, M. S. Hout, T. J. Hewitt, L. W. Lund, S. A. Heinrich, P. Litwak, F. R. Walters, G. D. Reeder, H. S. Borovetz and B. G. Hattler, "Development of a low flow resistance intravenous oxygenator," *ASAIO J*., vol. 43, pp. M725-M730, 1997.
[9] T. J. Hewitt, B. G. Hattler and W. J. Federspiel, "A mathematical model of gas exchange in an intravenous membrane oxygenator," *Ann. Biomed. Eng*,, vol. 26, pp. 166-178, 1998.
[10] J. D. Mortensen, "Intravascular oxygenator: A new alternative method for augmenting blood gas transfer in patient with acute respiratory failure," *Artif. Organs*, vol. 16, pp. 75-82, 1992.
[11] S. A. Conrad, "Major findings from the clinical trials of the intravascular oxygenator," *Arti. Organs*, vol. 18, pp. 846-863, 1994.
[12] T. T. Nguyen, J. B. Zwischenberger, W. Tao, D. I. Traber, D. N. Herndon, C. C. Duncan, P. Bush and A. Bidani, "Significant enhancement of carbon dioxide removal by a new prototype IVOX," *ASAIO J*., vol. 39, pp. M719-724, 1993.
[13] M. A. Woodhead, "Management of pneumonia," *Respir. Med*., vol. 86, pp. 459-469, 1992.
[14] S. N. Vaslef, L. F. Mockros, R. W. Anderson and R. J. Leonard, "Use of a mathematical model to predict oxygen transfer rates in hollow fiber membrane oxygenators," *ASAIO J*., vol. 40, pp. 990-996, 1994.
[15] H. M. Weissman and L. F. Mockros, "Gas transfer to blood flowing in coiled circular tubes," *J. Eng. Mech. Div. ASCM*, vol. 94, pp. 857-872, 1968.
[16] K. Tanishita, P. D. Richardson and P. M. Galletti, "Tightly wound coils of microporous tubing: progress with secondary flow blood oxygenator design," *Trans. ASME*, vol. 21, pp. 216-222, 1975.
[17] V. L. Streeter, E. B. Wylie and K. Bedford, *Fluid Mechanics*(9th ed.), New York, McGrew-Hill Inc., 1998.
[18] R. B. Bird, W. E. Stewart and E. N. Lightfoot, *Transport Phenomena*(2th ed.), New York, John Wiley & Sons Inc., 2002, pp. 675-677.
[19] M. Mulder, *Basic Principles of Membrane Technology*, AA Dordrecht, Kluwer Academic Publishers, 1996, pp. 418-422.
[20] W. L. Beek, K. M. K. Muttzell and J. W. van Heuven, *Transport Phenomena*(2th ed.), John Wiley & Sons(ASIA) PTE LTD, 1999, pp. 262-267.
[21] M. T. Snider, "Clinical Trails of an Intravenous Oxygenator in Patients with Adult Respiratory Distress Syndrome," *Anesthesoilogy*, vol. 77, pp. 855-863, 1972.
[22] P. J. Morin, C. Gosselin, R. Picard, M. Vincent, R. Giundoin and C. I. H. Nicholl, "Implantable Artificial Lung," *J. Thorac. Cardivasc. Surg.*, vol. 74, pp. 130-136, 1977.
[23] Y. Nosé, *Recommended Practice for Assessment of Hemolysis in Continuous Flow Blood Pump* West Conshohoken, P.A. American Society of Testing and Materials, 1998, pp. F04:40-41.
[24] K. Naito, K. Mizuguchi and Y. Nosé, "The Need for Standardizing the Index of Hemolysis," *Artif. Organs*, vol. 18, pp. 7-10, 1994.
[25] ISO/CD 199.2. Blood-gas Exchangers(Oxygenators) 1993. Document ISO/TC 150/SC2/WG/N 103.